

INVESTIGATION OF CAVITY DESIGNS ON VARIOUS AIRFOILS

YUVNEESH A/L VASUDEVAN

UNIVERSITI SAINS MALAYSIA

2021

INVESTIGATION OF CAVITY DESIGNS ON VARIOUS AIRFOILS

by

YUVNEESH A/L VASUDEVAN

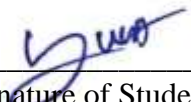
Thesis submitted in partial fulfilment of the requirement for the degree of

Bachelor of Aerospace Engineering

June 25

ENDORSEMENT

I, Yuvneesh A/L Vasudevan, hereby declare that I have checked and revised the whole draft of the dissertation as required by my supervisor.



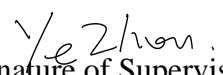
(Signature of Student)

Date:
6 July 2020



(Signature of Supervisor)

Name:
PM. Ir. Ts. Dr. Parvathy
Rajendran
Date:
6 July 2020

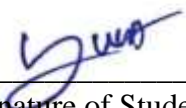


(Signature of Supervisor)

Name: Zhou Ye
Date: 6/7/2021

DECLARATION

This thesis is the result of my own investigation, except where otherwise stated and has not previously been accepted in substance for any degree and is not being concurrently submitted in candidature for any other degree.



(Signature of Student)

Date:
6 July 2020

ACKNOWLEDGEMENT

First and foremost, thanks to God for giving me the strength and blessing to complete my final year project. I also like to express my sincere gratitude to everyone who has supported and assisted me in finishing this project.

I would like to take this opportunity to thank my supervisor, Ir. Dr Parvathy Rajendran, for her constant guidance on my final year project from the beginning to the end of the semester, and her patience, insightful comments, excitement, and vast knowledge. This project would not have been possible without her encouragement and guidance.

Besides my supervisor, I would like to express my gratitude to my parents for their love, care, and prayers. In addition, I would like to thank my pals, Aaron and Nhaganthiran, for their unwavering support and encouragement when things became tough.

INVESTIGATION OF CAVITY DESIGNS ON VARIOUS AIRFOILS

ABSTRACT

Aerodynamic efficiency loss in airfoils is primarily due to the increased drag caused by boundary layer separation, especially at low Reynolds number. To reenergise the boundary layer and delay flow separation, cavities are introduced on the suction side of the airfoil. A cavity is a passive flow controller used to overcome a higher adverse pressure gradient and energise the low momentum boundary layers near the airfoil surface. In this paper, a total of 6 different airfoils is chosen to study the effect of the cavity and its design specification in term of size, shape, location, and number. The modified airfoils will be constructed in SOLIDWORKS and tested in PROFILI software which uses the XFOIL interface to calculate the airfoil's lift coefficient (C_l), drag coefficient (C_d), lift -to- drag ratio (l/d). It was found that the Clark y benefits the most when the cavity is introduced on the airfoil's suction side. Among the four different oval shapes, Oval Os provides a better l/d for Clark y, GEMINI and E387 airfoils, where the l/d increase by 11.41%, 1.22% 0.015%, respectively. Besides that, among the four different sizes, the cavity with 0.01 w/c gives the best aerodynamic performance to Clark y airfoil where the l/d of the airfoil is increased 9.03%. Apart from ^{the Clark y} ~~the Clark y~~ airfoil, the cavity with 0.01w/c also helps to reduce the C_d of GEMINI. E387 and NLF0416 by 4.80%, 6.42% and 4.59% respectively. From the analysis on the number of cavities, it was found that the single cavity works better for some of the airfoils, especially for Clark y airfoil. Moreover, for the multipole cavity, the C_d of the GEMINI, NLF 0416 and E387 airfoils is reduced; unfortunately, the airfoil's C_l also decreases, affecting the aerodynamic performance.

PENYELIDIKAN REKABENTUK Rongga PADA PELBAGAI AIRFOIL

ABSTRAK

Kehilangan kecekapan aerodinamik dalam bidang udara terutamanya disebabkan oleh peningkatan pekali seret yang disebabkan oleh pemisahan lapisan sempadan, terutama pada bilangan Reynolds yang rendah. Untuk menghidupkan kembali lapisan sempadan dan melambatkan pemisahan aliran, rongga diperkenalkan di bahagian penyedut udara. Rongga adalah pengawal aliran pasif yang digunakan untuk mengatasi kecerunan tekanan merugikan yang lebih tinggi dan memberi tenaga pada lapisan had momentum rendah berhampiran permukaan udara. Dalam makalah ini, sebanyak 6 jenis pesawat udara yang dipilih dipilih untuk mengkaji kesan rongga dan spesifikasi reka bentuknya dari segi ukuran, bentuk, lokasi, dan jumlahnya. Foil udara yang diubah akan dibina dalam SOLIDWORKS dan diuji dalam perisian PROFILI yang menggunakan antara muka XFOIL untuk mengira pekali angkat (Cl), pekali seret (Cd), nisbah angkat-ke-seret (l/d). Didapati bahawa Clark y memberi manfaat paling besar apabila rongga diperkenalkan di bahagian hisap pesawat udara. Di antara empat bentuk bujur yang berbeza, Oval Os memberikan l/d yang lebih baik untuk udara Clark y, GEMINI dan E387, di mana l/d meningkat masing-masing sebanyak 11.41%, 1.22% dan 0.015%. Di samping itu, di antara empat ukuran yang berbeza, rongga dengan $0,01 w/c$ memberikan prestasi aerodinamik terbaik untuk Clark y udara yang mana l/d dari bahagian udara meningkat 9.03%. Selain dari udara Clark y, rongga dengan $0,01 w/c$ juga membantu mengurangkan Cd GEMINI, E387 dan NLF0416 masing-masing sebanyak 4,80%, 6,42% dan 4,59%. Daripada analisis jumlah rongga, didapati bahawa rongga tunggal berfungsi dengan lebih baik untuk sebilangan rongga udara, terutamanya untuk kiriman udara Clark y. Lebih-lebih lagi, untuk rongga multipol, Cd GEMINI, NLF 0416 dan E387 dikurangkan; malangnya, Cl pesawat juga menurun, yang mempengaruhi prestasi aerodinami

Table of Contents

ENDORSEMENT.....	i
DECLARATION	ii
ACKNOWLEDGEMENT.....	iii
INVESTIGATION OF CAVITY DESIGNS ON VARIOUS AIRFOILS	iv
ABSTRACT.....	iv
PENYELIDIKAN REKABENTUK Rongga PADA PELBAGAI AIRFOIL.....	v
ABSTRAK.....	v
LIST OF FIGURES	ix
LIST OF TABLES	xii
LIST OF SYMBOLS	xiii
CHAPTER 1: INTRODUCTION	1
1.1 Overview	1
1.2 Problem Statement	4
1.3 Research Objective.....	5
1.4 Research Scope	5
1.5 Thesis Layout	6
CHAPTER 2: LITERATURE REVIEW	7
2.1 Introduction.....	7
2.2 Cavity Design Parameters.....	9
2.2.1 Number of Cavity	9
2.2.2 Shape of Cavity.....	10
2.2.3 Size of Cavity.....	11
2.2.4 Position of Cavity	13

CHAPTER 3: METHODOLOGY	17
3.1 Introduction.....	17
3.2 Airfoil Design	19
3.2.1 SOLID WORK.....	21
3.3 Airfoil Analysis.....	25
3.3.1 XFOIL.....	25
3.3.2 Panel method.....	26
3.3.3 PRFOILI	29
3.3.4 Operating parameter.....	31
CHAPTER 4: RESULT AND DISCUSSION.....	33
4.1 Validation.....	33
4.2 Shape of Cavity.....	37
4.2.1 Oval Od.....	37
4.1.2 Oval Sc.....	40
4.1.3 Oval Om.....	43
4.1.3 Oval Os	46
4.2 Size of Cavity.....	51
4.2.1 w/c=0.01	51
4.2.2 w/c=0.015	54
4.2.3 w/c=0.02	57
4.2.3 w/c=0.025	59
4.3 Number of Cavity	64
4.3.1 Single cavity.....	64

4.3.2 Double cavity	67
4.3.3 Triple cavity	70
4.3.4 Quadruple cavity	73
4.4 Position of Cavity	78
4.5 Summary of Findings based on the airfoils.	83
CHAPTER 5: CONCLUSION AND RECOMMENDATION	93
5.1 Recommendations for Future Works	94
REFERENCE.....	95

LIST OF FIGURES

		Page
Figure 1.0	Airfoil nomenclature	1
Figure 1.1	Boundary layer separation over the top surface of a wing	3
Figure 2.1	The delay of flow separation due to golf ball dimple	8
Figure 2.2	The three selected dimple configurations	11
Figure 2.3	Dimple dimensions	12
Figure 2.4	The schematic of cavity geometry	12
Figure 3.1	Dimple dimensions: dimple width (w), dimple depth (d)	20
Figure 3.2	The outline of E387 airfoil	22
Figure 3.3	Oval 3 cavity with fillet size c/10	23
Figure 3.4	Airfoil E387 with a triple cavity at 15c, 30c, 60c	24
Figure 3.5	The new polar coordinates created on the E387 airfoil	25
Figure 3.6	The panel alignment over the E387 airfoil	27
Figure 3.7	PROFILI GUI interface	30
Figure 3.8	The modified E387 airfoil's preview and imported coordinate data	31
Figure 4.1	Graph of Lift coefficient against Angel of attack(J5012)	33
Figure 4.2	Graph of Lift coefficient against Angel of attack (Clark Y)	33
Figure 4.3	Graph of Lift coefficient against Angel of attack(E387)	34
Figure 4.4	Graph of Lift coefficient against Angel of attack (NLF-0416)	34
Figure 4.5	Graph of Lift coefficient against Angel of attack (Falcon)	35
Figure 4.6	Graph Lift coefficient against Angel of attack (Gemini)	35
Figure 4.7	Graph of Percentage difference Cl Vs α for Oval Od cavity	37
Figure 4.8	Graph of Percentage difference Cd Vs α for Oval Od cavity	38
Figure 4.9	Graph of Percentage difference l/d Vs α for Oval Od cavity	38
Figure 4.10	Graph of Percentage difference Cl Vs α for Oval Sc cavity	40
Figure 4.11	Graph of Percentage difference Cd Vs α for Oval Sc cavity	40
Figure 4.12	Graph of Percentage difference l/d Vs α for Oval Sc cavity	41

Figure 4.13	Graph of Percentage difference C_l Vs α for Oval O_m cavity	43
Figure 4.14	Graph of Percentage difference C_d Vs α for Oval O_m cavity	43
Figure 4.15	Graph of Percentage difference l/d Vs α for Oval O_m cavity	44
Figure 4.16	Graph of Percentage difference C_l Vs α for Oval O_s cavity	46
Figure 4.17	Graph of Percentage difference C_d Vs α for Oval O_s cavity	46
Figure 4.18	Graph of Percentage difference l/d Vs α for Oval O_s cavity	47
Figure 4.19	Graph of Percentage difference C_l Vs α for 0.01 w/c cavity	51
Figure 4.20	Graph of Percentage difference C_d Vs α for 0.01 w/c cavity.	51
Figure 4.21	Graph of Percentage difference l/d Vs α for 0.01 w/c cavity.	52
Figure 4.22	Graph of Percentage difference C_l Vs α for 0.015 w/c cavity	54
Figure 4.23	Graph of Percentage difference C_d Vs α for 0.015 w/c cavity.	54
Figure 4.24	Graph of Percentage difference l/d Vs α for 0.015 w/c cavity.	55
Figure 4.25	Graph of Percentage difference C_l Vs α for 0.02 w/c cavity	57
Figure 4.26	Graph of Percentage difference C_d Vs α for 0.02w/c cavity.	57
Figure 4.27	Graph of Percentage difference l/d Vs α for 0.02 w/c cavity.	58
Figure 4.28	Graph of Percentage difference C_l Vs α for 0.025 w/c cavity.	59
Figure 4.29	Graph of Percentage difference C_d Vs α for 0.025 w/c cavity.	59
Figure 4.30	Graph of Percentage difference l/d Vs α for 0.025 w/c cavity.	60
Figure 4.31	Graph of Percentage difference C_l Vs α for single cavity.	64
Figure 4.32	Graph of Percentage difference C_d Vs α for single cavity.	64
Figure 4.33	Graph of Percentage difference l/d Vs α for single cavity.	65
Figure 4.34	Graph of Percentage difference C_l Vs α for Double cavity.	67
Figure 4.35	Graph of Percentage difference C_d Vs α for Double cavity.	67
Figure 4.36	Graph of Percentage difference l/d Vs α for Double cavity.	68
Figure 4.37	Graph of Percentage difference C_l Vs α for Triple cavity.	70
Figure 4.38	Graph of Percentage difference C_d Vs α for Triple cavity.	70
Figure 4.39	Graph of Percentage difference l/d Vs α for Triple cavity.	71
Figure 4.40	Graph of Percentage difference C_l Vs α for Quadruple cavity.	73
Figure 4.41	Graph of Percentage difference C_d Vs α for Quadruple cavity.	73
Figure 4.42	Graph of Percentage difference l/d Vs α for Quadruple cavity.	74
Figure 4.43	Graph of Average Percentage Difference of C_l against the Position of Cavity	78

Figure 4.44	Graph of Average Percentage Difference of Cd against the Position of Cavity	78
Figure 4.45	Graph of Average Percentage Difference of l/d against the Position of Cavity	79

LIST OF TABLES

		Page
Table 1.0	Aerodynamic performance Grooved airfoil	15
Table 2.0	Design Specification of Groove	16
Table 3.0	Airfoil Selection	18
Table3.1	The summary table of cavity design parameter	20
Table3.2	The summary table of cavity shape and their aspect ratio	21
Table3.3	The Combination of cavity position	23
Table3.4	The operating parameters and XFOIL settings	32
Table4.1	The percentage error difference between experiment and XFOIL results	36
Table4.2	The summary of airfoil's aerodynamic performance when tested with different cavity shape.	49
Table4.3	The summary of airfoil's aerodynamic performance when tested with different cavity size.	62
Table4.4	The summary of airfoil's aerodynamic performance when tested with different number of cavities.	76
Table4.5	The summary of airfoil's aerodynamic performance when tested with different position of cavities.	79-81
Table4.6	The summary of cavities performance based on the airfoils(shape).	83
Table4.7	The summary of cavities performance based on the airfoils(size).	85
Table4.8	The summary of cavities performance based on the airfoils (number of cavity).	87
Table4.9	The summary of cavities performance based on the airfoils(position)	89-91

LIST OF SYMBOLS

C_d	Coefficient of Drag
C_l	Coefficient of Lift
C_p	Pressure Coefficient
l/d	Lift to Drag ratio
Re	Reynold's number
w/c	Cavity ratio
d/w	Aspect ratio

CHAPTER 1: INTRODUCTION

1.1 Overview

An airfoil is a two-dimensional structure with curved surfaces that plays a major role in any fluid mechanics design application, such as a marine propeller, wind turbine, or aircraft wing. An airfoil generates a lifting force perpendicular to the airstream and a dragging force parallel to the airstream. The fundamental geometry of an airfoil is shown in Figure 1.

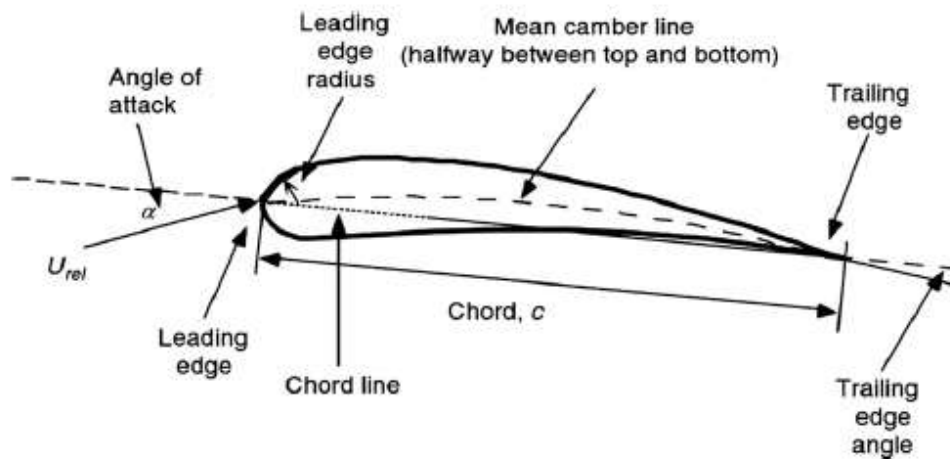


Figure 1.0: Airfoil nomenclature(Sayed et al., 2012)

The chord, camber, and thickness are the most significant characteristics of an airfoil profile. The leading edge is the forward point, while the trailing edge is the backward point. The chord line connects the leading and trailing edges, and the chord of an airfoil is the distance measured between the trailing and leading edges along the chord line. The mean camber line, measured perpendicularly from

the chord line, points midway between the upper and lower surfaces. The thickness of an airfoil is the distance between the top and lower surfaces measured perpendicular to the chord line, and it changes along the chord line. The maximum distance between the mean camber line and the chord line is known as camber. Maximum camber and thickness and their location along the chord line are key design elements for airfoils used to classify them.

Airfoils produce lift by displacing airflow and causing a net curve as the air is directed downwards. The air moving over the upper surface speeds up, while the air moving over the lower surface slows down. Bernoulli's principle can be used to calculate the lift generated in subsonic incompressible flow in terms of pressure. According to the Bernoulli equation, increasing airspeed relative to the airfoil's upper surface reduces pressure, while decreasing airspeed relative to the wing's bottom surface increases pressure(Anderson, 2005). A lift force is generated by the pressure difference between the two surfaces. As a result, the upper and lower surfaces are the suction and pressure surfaces, respectively.

Boundary layer separation is one of the critical issues that airfoils encounter. This phenomenon will result in significant energy loss and impact an airfoil's aerodynamic performance by reducing lift and raising drag. When the boundary layer encounters an unfavourable pressure gradient, the boundary layer separates. The adverse pressure gradient will diminish the momentum of the boundary layer, causing it to detach from the airfoil's surface. For a better understanding, a detailed view of the boundary layer separation over the top surface is shown in Figure 1.1.

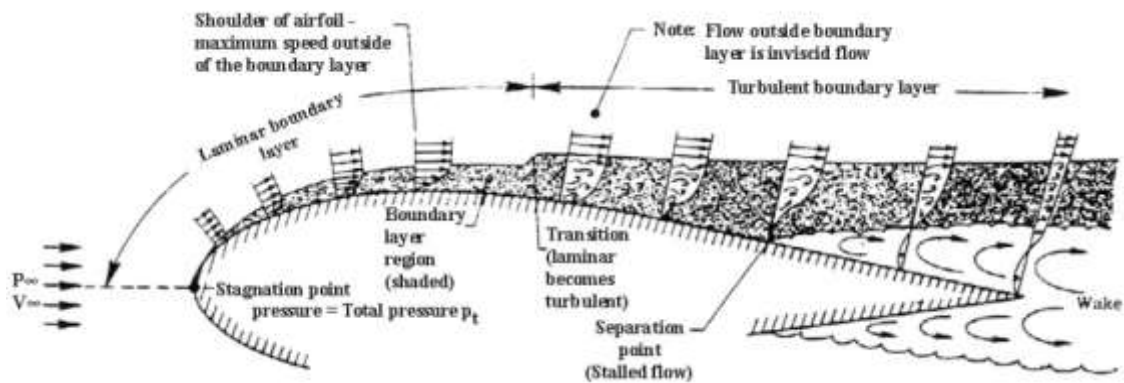


Figure 1.1: Boundary layer separation over the top surface of a wing

A boundary layer forms around it when an airfoil passes through a fluid, guiding its performance further. As long as the surface is smooth, the flow will remain laminar and eventually separate into layers. The flow detachment from the airfoil surface causes the wake behind the airfoil, where the flow takes the forms of vortices. The disconnected flow is reattached to the surface by infusing turbulence through the shear due to its natural adhesive nature.

One way to control the boundary layer separation is using boundary layer separation control or flow separation control. The main aim of this method is to create an array of small streamwise vortices that promote increased mixing between high-speed air in the mainstream and outer boundary layer with the low-speed air closer to the surface (Shan et al., 2008). Thus, the boundary layer is reenergised, delaying the flow separation (Fatahian et al., 2019). The flow separation control can be divided into active control and passive control. Both active and passive control achieve the desired change in the flow patent and boundary layer (Findanis, 2015, Joshi and Gujarathi, 2016). Active control requires energy and involves a control system, while passive control does not require

energy(Liu et al., 2020b). Active flow control focuses on developing the flow into a more desired path. For example, active control usually modifies the flow through blowing or suction or jets. Stored fluids are pumped and blown either tangential or vertical to the surface. But passive control does not use additional active devices but rather uses free stream air velocity (Kutty et al., 2017).

The main focus of this research is on passive control using a cavity on the top of the airfoil surface. The cavities are positioned on airfoils to modify the flow around them for greater aerodynamic performance. The Passive slots will be tested on the airfoil in terms of shape, size, number, position.

1.2 Problem Statement

The higher drag caused by boundary layer separation is the primary cause of the loss in aerodynamic efficiency. Cavities on the airfoil's upper surface, which is one of the passive flow controls, can be used to reenergise the boundary layer and delay flow separation. To overcome a higher adverse pressure gradient, the cavities will energise the low momentum layers near the airfoil surface without contributing extra energy(Ramzi et al., 2011). Because of their simplicity and cost-effectiveness, cavities remain the preferred option for low-speed applications such as MAVs, UAVs, low-speed turbines, and propellers.

Even though numerous studies is carried out on cavities, all the studies are mostly focus on symmetrical airfoils and more research is required for study the effect of different locations of cavity and an array of cavity on the airfoils. This

research aims to create several cavity designs and their effect on airfoils with different aerodynamic and physical properties, such as symmetrical, semi-symmetrical, laminar flow, reflex camber, high camber under camber, and flat bottom.

1.3 Research Objective

This research project intends to achieve the following goals to address the issues mentioned above:

- I. To investigate the effect of cavity designs in terms of various cavity size, shape, number, and position on different airfoils.
- II. To determine which type of airfoil benefits the most when the cavity is introduced.

1.4 Research Scope

The scope of the research is limited to a low Reynolds' number of 100.000 where six types of airfoils will be studied by introducing various cavities on the suction side of the airfoil at 15,30,45, and 60 percent of the airfoil chord length. In this paper, the cavity size is studied based on the cavity ratio (d/w , w : width, d : depth) ranging from 0.01- 0.025 with an increment of 0.05. The analysis is also conducted with different cavity ratio (w/c , w : width, c : chord length) starting from 0.01 till 0.25 with an increment of 0.05. All the modified airfoil will be numerically analyse using the PROFILI software.

1.5 Thesis Layout

The outline of the thesis is as follows: Chapter 2, Literature Review, presents the review on literature about surface modifier, cavity design parameters in term of the number of cavities, shape of the cavity, size of cavity and position of the cavity. Airfoils, airfoil design, panel method, XFOIL, PROFIL and operating parameters in Chapter 3, Methodology. Chapter 4, Results and Discussions, displays and analyses result of all six airfoils with different cavity shape (Oval OS, Oval Om, Oval Sc, Oval OS), different cavity size ($w/c=0.1, 0.15, 0.02, 0.025$), various number of the cavity (single cavity, double cavity, triple cavity and quadruple cavity) and various position of the cavity. Conclusions and recommendations are presented in Chapter 5, Conclusions and Recommendations.

CHAPTER 2: LITERATURE REVIEW

2.1 Introduction

The interest in low-Reynolds number flow over airfoils has been reignited by a recent spike in activity linked to the design of Micro-Air-Vehicles (MAV), Unmanned Air Vehicle (UAV), wind turbine etc. Boundary layer separation can have undesirable consequences in low Reynolds number flows, such as a reduction in lift, an increase in drag, a decrease in aircraft stability, vibration, and noise. Thus, various leading-edge, surface, and trailing edge modifiers are frequently attempted to enhance airfoil's aerodynamic efficiency (L/D).

Surface modifiers are passive control systems that generate turbulence by forming vortices, which delays boundary layer separation and reduces pressure drag while simultaneously increasing stall angle. It reduces pressure drag while also increasing the aircraft's overall lift. Various types of surface modifiers are now being investigated to increase the aircraft's performances. For example, vortex generators (VG) are passive surface modifiers placed over the wing surface to improve the lift to drag ratio by adding extra momentum to the boundary layer and delaying flow separation (Jumahadi et al., 2018).

Besides that, slots/cavities/dimples represent one of the older methods to control boundary layer. Cavity drag reduction is a reasonably inexpensive and effective passive control approach. The cavity/dimple method is inspired by the concept of a dimple on golf balls. The dimple effect of the golf ball inspired the

researcher because of its extended range and trajectory and the massive resistance to airflow around the dimpled surface compared to the smooth surface. The use of dimples on a golf ball has increased lift and range by delaying boundary layer separation. Figure 2.1 show the delay of flow separation due to golf ball dimple.

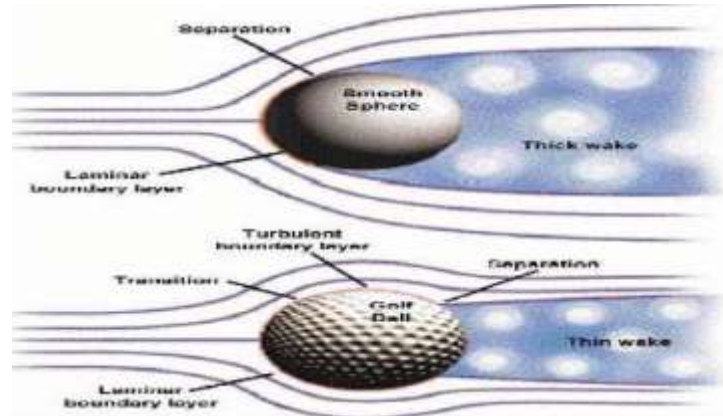


Figure 2.1: The delay of flow separation due to golf ball dimple
(Mustak and Ahmed, 2017).

In the same way, modifying the surface of an airfoil with cavity/dimples increases its aerodynamics (Mustak and Ahmed, 2017). Study shows that the airfoil with dimples will have significantly less drag than a standard airfoil. The introduction of dimples to an aircraft wing will induce turbulence by producing vortices, delaying boundary layer separation, lowering pressure drag and increasing stall angle (Livya et al., 2015).

2.2 Cavity Design Parameters

2.2.1 Number of Cavity

A numerical simulation was carried out to investigate the effect of the passive control method, with different shapes and number of the cavity, applied to the upper surface of a NACA0012 airfoil, on the pressure field at Reynolds number of 9.0×10^6 . (Manshadi and Rabani, 2016). The number of slots placed on the airfoil's upper surface is decided based on the length-to-spacing ratio (W/P). It was found that, at all length-to-spacing ratios, the drag force coefficient decreases, which increases the aerodynamic efficiency. Simultaneously, the lift force coefficient is reduced, which suppresses the upward trend in aerodynamic efficiency and even lowers its value at large length-to-spacing ratios.

Besides that, (Wang and Sun, 2000) studied implementing multiple slots at low speeds to control boundary-layer separation on a thick airfoil efficiently. He tested airfoil (Naca 0012) with multiple slots (10 slots) and a single slot at a low Reynolds number of 3.0×10^6 . In his conclusion, he states that multiple-slot blowing creates a significantly bigger C_l and a considerably smaller C_D than single-slot blowing. The airflow over a multi-slot airfoil is sustained and does not separate, whereas the airflow over a single slot airfoil separates near the trailing edge.

2.2.2 Shape of Cavity

(Mustak et al., 2015) has experimented with three wooden Airfoil Models with outward and inward dimples and without dimples. According to the experiment results, the use of dimples on the airfoil's upper surface can delay flow separation on the airfoil, and the lift force and stall AOA are also significantly increased. Both the outward and inward dimpled models have lower drag than the plain airfoil variant. Outward dimpled airfoils have the least drag compared to inward dimpled airfoils.

A numerical study is carried out to observe the effect of different cavity shape on the aerodynamic performance of a NACA 4415 airfoil. It was found that the rectangular cavity outperforms the arc cavity in terms of aerodynamic performance, as the rectangular design more effectively confines flow motion inside the cavity (Liu et al., 2020a). Besides that, (Chullai et al., 2019) use V-shaped dimple to increase the lift coefficient near the stalling angles of NACA 0012 symmetrical airfoil. In his conclusion, he mentioned that V-dimple is effective in delaying the flow separation.

(Baweja et al., 2016) has researched inward hemispherical, outward hemispherical, and composite inward configurations to establish the highest attainable effectiveness in delaying boundary layer separation at the trailing edge. Figure 2.2 shows the selected dimple configuration. Based on the results, the outward semi-spherical dimples were effective inflow attachment. Still, they reduced overall wing lift and increased drag due to creating a high-pressure area at

the dimple boundary. On the other hand, inward dimples are more effective since they improve overall wing lift without increasing overall drag. Overall, the composite shaped inward dimples demonstrated the most efficient flow regime, creating a low-pressure area inside the dimple to produce suction force for flow attachment.

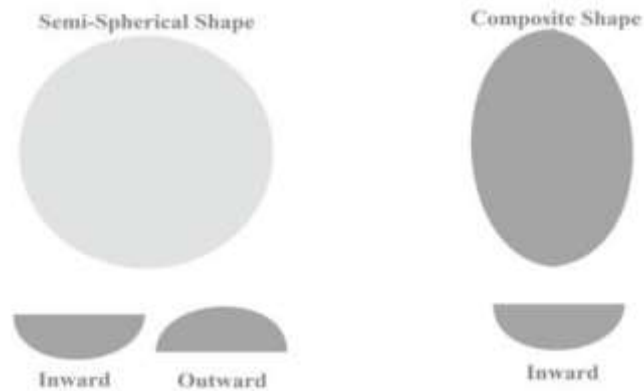


Figure 2.2: The three selected dimple configurations(Baweja et al., 2016)

2.2.3 Size of Cavity

A numerical study was carried out to study the effect of surface groove on the aerodynamic performance of a NACA 4415 airfoil for low Reynolds number at (5.0×10^5) (Liu et al., 2020a). In this study, the cavity geometry parameter refers to the recess depth ratio (h/δ , h : cavity recess depth, δ : baseline boundary layer thickness) and aspect ratio (h/w , h : cavity recess depth, w : cavity width). Figure 2.3 shows the cavity dimension. The airfoil is tested with five different recess depth ratio (0.5,1.0,1.2,1.5,2.0) and two aspect ratio (0.1-0.15). The study concludes that a smaller aspect ratio of recess depth to cavity width is necessary to capture the vortex for a shallow recess depth. Still, a greater aspect ratio can

stabilise the vortex for a deep recess. Moreover, the lift to drag ratio increases and gives better aerodynamic performance when the recess depth ratio $h/\delta = 1.2$ and aspect ratio $h/w = 0.1-0.15$.

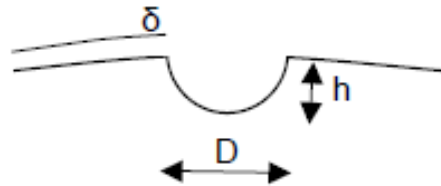


Figure 2.3: Dimple dimensions(Robarge et al., 2004)

In another study, a computation analysis was carried out on NACA 0015 airfoil with different cavity geometry to improve the performance of wind blade(Seo and Hong, 2016). The analysis was conducted at the 7° angle of attack with various h/d (0.1 – 1.4), l/δ (-0.5-0.5) and h/δ (0.6-1.0) where the h is the depth of the cavity, d is the width of cavity ratio, l is the length between the end of cavity and separation point, δ is the thickness of boundary layer. Figure 2.4 shows the schematic of cavity geometry. The highest improvement in lift to drag ratio was 15.3 percent, under the circumstances $h/\delta = 1.0$, $h/d = 0.12$, and $l/\delta = -0.5$ at Reynolds number $Re = 360k$. He also claims that the cavity's shape helped recover velocity around the airfoil wall, improving wind blade performance.

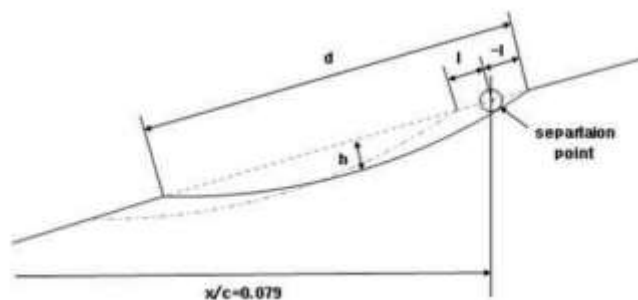


Figure 2.4: The schematic of cavity geometry(Seo and Hong, 2016)

2.2.4 Position of Cavity

(Lv et al., 2020) in his numerical study, he found out that the cavity applied on the suction side improves the lift, reduces the drag, and at the same time delays the stall angle while the cavity used on the pressure side, show poor performance. Besides that, (Liu et al., 2020a) mentioned in their journal that surface groove with the optimum geometry position increases the aerodynamic lift-to-drag ratio by approximately 50% at the design angle of attack equal to 10° . The size of potential vortices produced within the cavity and the thickness of the local boundary layer are affected by the cavity position.

In numerical analysis, dimples were put at three distinct chordwise locations, namely, 75%, 50% and 25% of chord and compared to a smooth airfoil. It was discovered that an airfoil with a dimple at 75% of the chord length successfully regulates boundary layer separation and boosts the airfoil's maximum Lift Coefficient by 1-2%. In addition, the airfoil with a dimple at 75% of the chord length raises the stall angle by 2 degrees because the dimple's rear face blocks reverse flow (MR, 2017).

A similar study has been done by (Saraf et al., 2017), where the author investigated the aerodynamic properties of the NACA0012 airfoil with and without a dimple. At a constant airspeed of 7.3 m/s and varied attack angles, a single inward dimple was used on the airfoil's upper surface (75 percent, 50 percent, 25 percent, and 10% of the chord length from the leading edge). According to the findings,

compared to a smooth airfoil, the presence of dimples at 75 percent of the chord boosted lift by 7% and reduced drag by 3%.

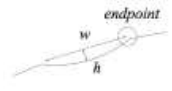
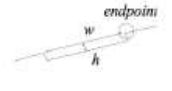
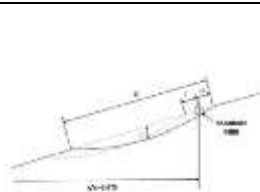
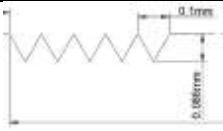
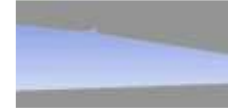
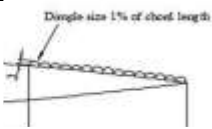
Furthermore, (Rasal and Katwate, 2017) numerically investigated the characteristics of the NACA 0012 airfoil without and with dimples. At a speed of 6 m/s, 3 mm circular dimples were applied to the airfoil's upper surface at 1 percent and 70% chord length from the leading edge. The lift to drag ratio coefficient was computed numerically at various angles of attack ranging from 0 to 23 degrees. The results showed that adding dimples enhances the lift coefficient while also increasing the drag coefficient as the angles of attack rise.

Table 1.0 and 2.0 shows the summary of the literature review. Based on the literature reviews, only a few studies focus on cavity locations and the number of cavities. Moreover, only a few researchers tested the cavity on different airfoil types and observed the cavity effect on them. Thus, in this study, six airfoil types will be selected and modified with varying shapes of cavity, position, sizes, and numbers to study the cavity effect on the airfoils.

Table 1.0 Aerodynamic performance of airfoil with cavity

Type	Reynolds number	Variant	Aerodynamic performance				
			Cl base	Cd base	Cl max	Cd max	l/d max
NACA4415 (Mustak et al., 2015)	-	Inward dimple	1.0 at α 16	0.36 at α 28	1.4 at α 16	0.41 at α 28	↑ 5.7 at α 10
		Outward dimple	1.0 at α 16	0.36 at α 28	1.36 at α 16	0.37 at α 28	↑ 5.2 at α 10
NACA4415 (Liu et al., 2020b)	5.0×10^5	Arc	Overall, the airfoil with a cavity has ↑ cl and ↓ cd. For instance, cl at α 10 is rise from 1.25 to 1.4 and, cd at α 10 is reduce from 0.03 to 0.022. The aerodynamic performance show ↑ 50% improvement.				
		Rectangular					
NACA 0012 (Chullai et al., 2019)	3×10^6	V-shape	Cl value of dimpled airfoil ↑ and Cd value of dimpled airfoil ↓ from α 14 onwards. Aerodynamic efficiency ↑ by 13.25% at 14°, 47% at 16° and 18.24% at 18°.				
NACA 22112 (Baweja et al., 2016)	6×10^6	Inward composite dimple	↑ in lift and significant ↓ in drag, at higher angle of attack				
NACA 0015 (Seo and Hong, 2016)	3.6×10^5	Arc	-	-	-	-	↑ 15.3 at α 7
NACA 0012 (Lv et al., 2020)	1.17×10^7	Suction side (triangular Concave)	~1.6 at α 14°	~0.33 at α 15°	↓ ~1.55 at α 14°	↓ ~0.20 at α 15	↓ 20 at α 5
NACA 4415 (MR, 2017)	3×10^6	Triangular	1.40 at α 20	1.46 at α 20	↑ 1.47 at α 20	↓ 1.45 at α 20	-
NACA0012 (Saraf et al., 2017)	-	Inward dimple/cavity	1.20 at α 14	-2.38 at α 14	↑ 1.29 at α 14	↓ -2.41 at α 14	-
NACA0012 (Rasal and Katwate, 2017)	-	outward dimple	0.3 at α 23	0.13 at α 23	↑ 0.75 at α 23	↑ 0.31 at α 23	-

Table 2.0 Design Specification of Cavity

Reference	Figure (Reference)	Design Specification			
		Location	Shape	Size	Number of slots
1 (Mustak et al., 2015)		-	Inward and outward dimple	d=1.5mm	13 over the wing
2 (Liu et al., 2020b)		Leading edge	Arc	h/δ =0.5-2.0 h/w=0.1-0.15	1
			Rectangular		
3 (Chullai et al., 2019)		At 80% of chord length (0.8c)	V-shape	h/w=0.86 L=0.0089	1
4 (Baweja et al., 2016)		0.68c from leading edge	Inward and outward dimple	d=40mm,60mm,80mm,100mm	For (d<60) =15 For (d>60) =12
5 (Seo and Hong, 2016)		Leading edge	Arc	h/δ=0.6-1.0, h/d=0.1-1.4, l/δ=-0.5-0.5	1
6 (Lv et al., 2020)		Suction side & Pressure side (0.2m from the Leading edge)	Triangular	0.1mm x 0.086mm (1)	30
7 (MR, 2017)		75c ,50c,25c	Triangular	d x h=3mm x 1.5mm	1
8 (Saraf et al., 2017)		75c ,50c,25c,10c	Inward and outward dimple	d=0.02% c	1
9 (Rasal and Katwate, 2017)		70 c	Rectangular and circular outward dimple	d=1% c	15

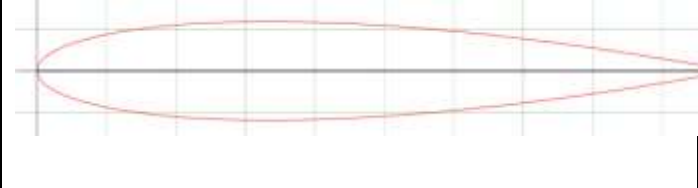
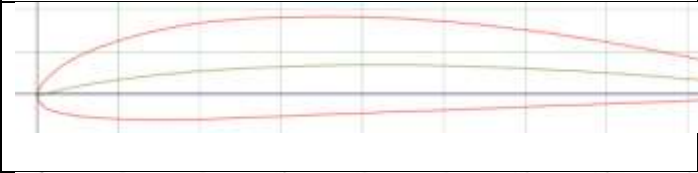
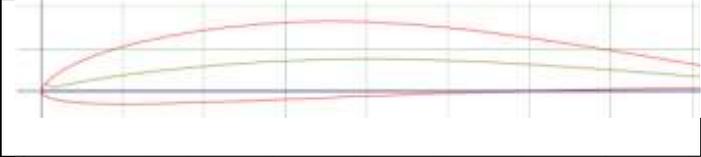
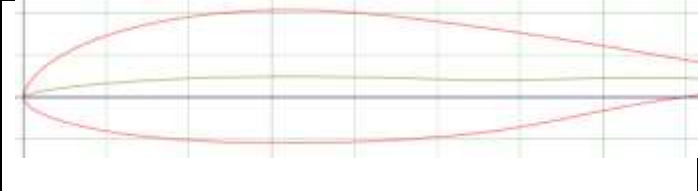
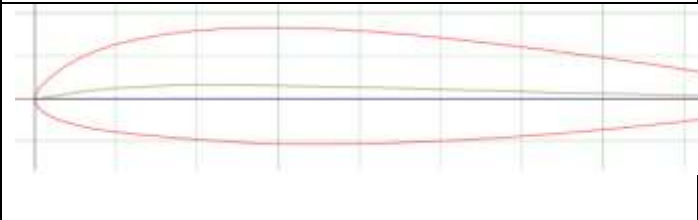
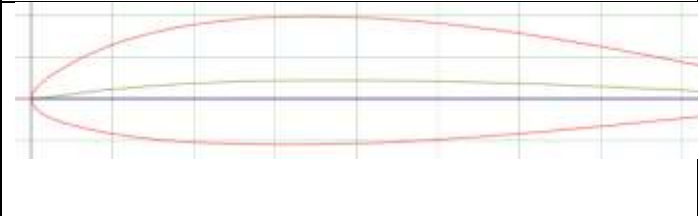
CHAPTER 3: METHODOLOGY

3.1 Introduction

In this paper, a total of 6 different airfoils is chosen to study the effect of the cavity and its design specification in term of size, shape, location, and number. The numerical analysis will be conducted with the aid of software called PROFILI. The modified airfoils will be constructed in SOLIDWORKS and tested in PROFILI software which uses the XFOIL interface to calculate the airfoil's lift coefficient (C_l), drag coefficient (C_d), Lift -to- drag ratio (L/D) and pitching moment coefficient (C_m). Then, the simulated results will save in Microsoft Excel to construct graphs and data tables to discuss the simulated results.

Six different airfoils with different aerodynamic performance are selected to study the cavity's effect and design specification. Table 3.0 show all the 6-airfoil geometries and their categories. For validation, all the airfoil's base design numerical results obtained from the XFOIL are compared with actual experiment results conducted in a wind tunnel (Selig, 1995, MARCHMAN, 1984, McGhee and Walker. Graph 3.1 to 3.6 show the comparison between the numerical results and experimental data.

Table 3.0 Airfoil Selection

No	Airfoil name	Airfoil type	Airfoil Image
1	J5012 (Selig, 1995)	Symmetrical	
2	Clark y (MARCHM AN, 1984)	Flat bottom/low camber	
3	E387 (McGhee, 1988)	Reflex camber	
4	NLF 0416 (Somers, 1997)	Laminar flow airfoil	
5	Falcon (Selig, 1995)	Semi symmetrical	
6	GEMINI (Selig, 1995)	High camber	

3.2 Airfoil Design

All the six types of airfoils will be studied by introducing oval shape cavities with a various aspect ratio (d/w , d : depth, w : width) on the upper surface of the airfoil at 15,30,45, and 60 percent of the airfoil chord length, c . The oval shape cavity was chosen in order to investigate the cavity's depth influence on the airfoil and how it affects the airfoil's aerodynamic performance.

According to(Liu et al., 2020a, Seo and Hong, 2016) and other researchers, the cavity size is study based on the cavity's ratio, aspect ratio and recess depth ratio. In this paper, the cavity size is studied based on the cavity ratio ranging from 0.01- 0.025 with an increment of 0.05. The analysis is also conducted with different cavity ratio (w/c , w : width, c : chord length) starting from 0.01 till 0.25 with an increment of 0.05. The detailed view of the cavity dimension is shown in figure 3.1.

Based on (Wang and Sun, 2000), multiple slot/cavity airfoil is sustained and improves airfoil performance compared to single cavity airfoil. Thus, in this paper, multiple cavity airfoil will be tested with various combinations of cavity position to study the effect of numerous cavities on the airfoil and how it works for a different type of airfoil. A total of 1440 airfoil designs is created in the SOLIDWORKS software. Table 3.2 and 3.3 show the summary of cavity design parameters and the dimensions of the cavity shapes.

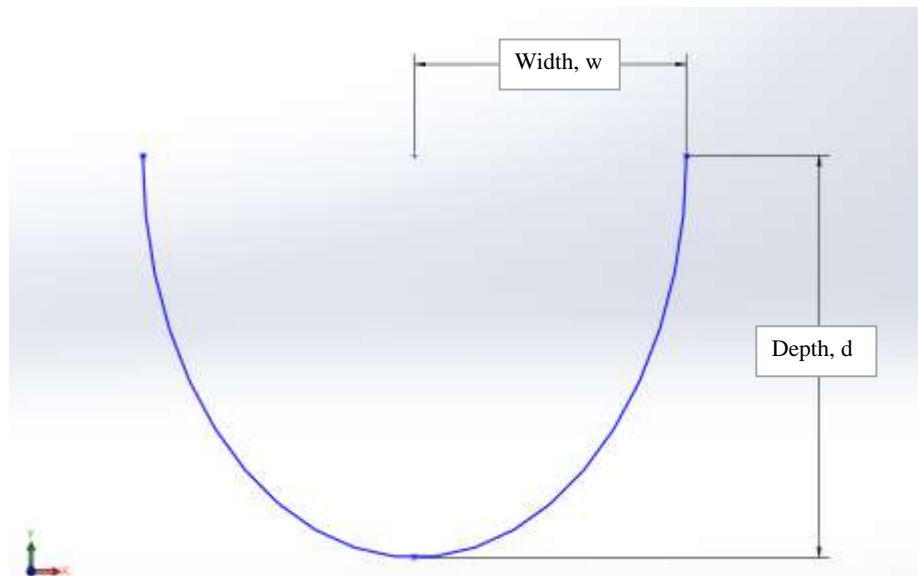
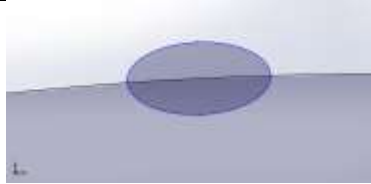
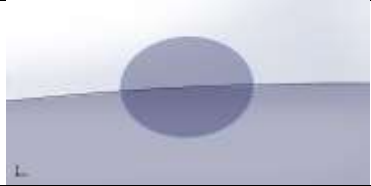
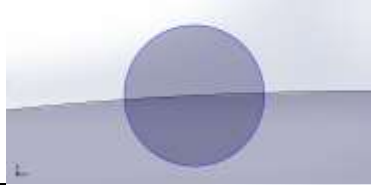
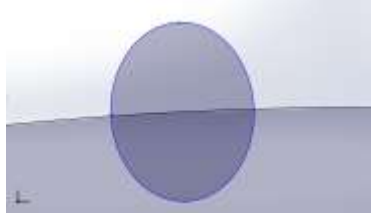


Figure 3.1. Dimple dimensions: dimple width (w), dimple depth (d)

Table3.1: The summary table of cavity design parameter\

Shapes	Location	Cavity ratio	Number of slots
Oval 1(Os)	15C,30C,45C, 60C	w/c=0.01,0.15,0.02,0.025	1,2,3,4
Oval 2(Om)			
Oval 3/ Semicircle (Sc)			
Oval 4 (Od)			

Table3.2: The summary table of cavity shape and their aspect ratio

Shapes	Figure	Aspect ratio, d/w	
		Width, w	Depth, d
Oval 1(Os)		4	2
Oval 2(Om)		4	3
Oval 3 / Semicircle (Sc)		4	4
Oval 4 (Od)		4	5

3.2.1 SOLID WORK

The airfoil geometry is created in SOLIDWORK by entering the airfoil's existing polar coordinates. The airfoil's polar coordinates are obtained from the XFOIL database. The chord length of each airfoil is kept constant at 100mm. All the polar coordinates of the six airfoils are included in the appendix section. Figure 3.2 show the drawing process of airfoil E387 using the airfoil's polar coordinates in the SOLIDWORKS workstation for further modification. The shape of the airfoil is generated using the curve tool found in the SOLIDWORKS.

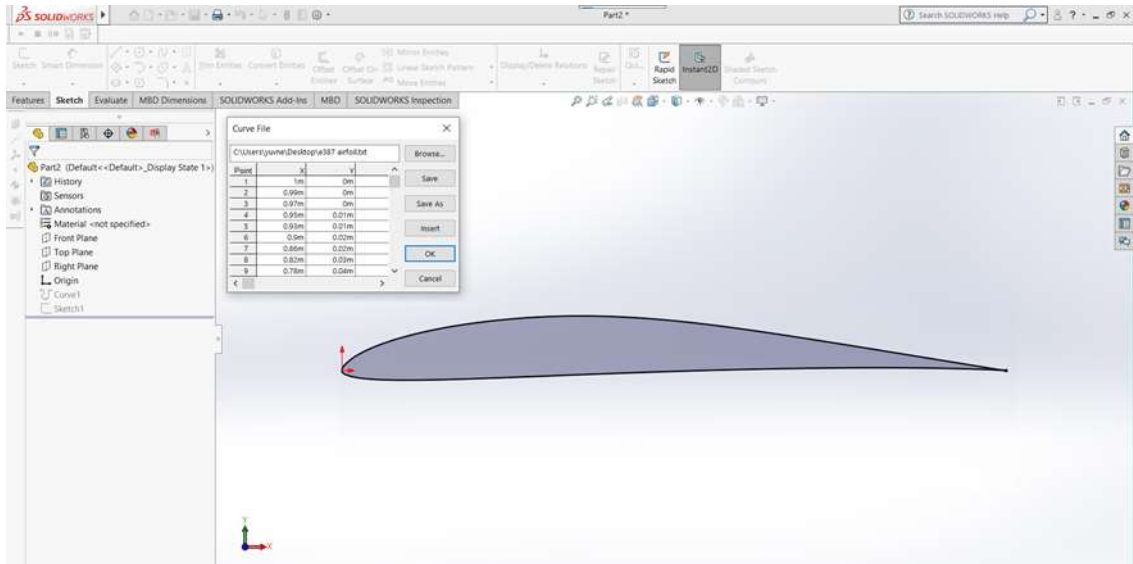


Figure3.2: The outline of E387 airfoil

After generating the airfoil's outline, the cavity design is sketched on the airfoil's upper surface at 15%, 30%, 45%, and 60% of airfoil chord length. Moreover, a total of 15 combinations of cavity number and its position is created on an airfoil. The cavity combination list is shown in the table below. After that, the sketched cavity design is trimmed using the trim tool available in SOLIDWORK. Furthermore, based on the journal (Merryisha and Rajendran, 2019), all the cavity design is added with a fillet size of $c/10$ on both ends of the cavity to improve the flow regime and prevent sudden shock waves. The preview of the cavity design with a fillet is shown in the figure3.3.

Table3.3: The Combination of cavity position

No	Combination of cavity position
1	15c
2	15c30c
3	15c30c45c
4	15c30c45c60c
5	15c30c60c
6	15c45c
7	15c45c60c
8	15c60c
9	30c
10	30c45c
11	30c45c60c
12	30c60c
13	45c
14	45c60c
15	60c

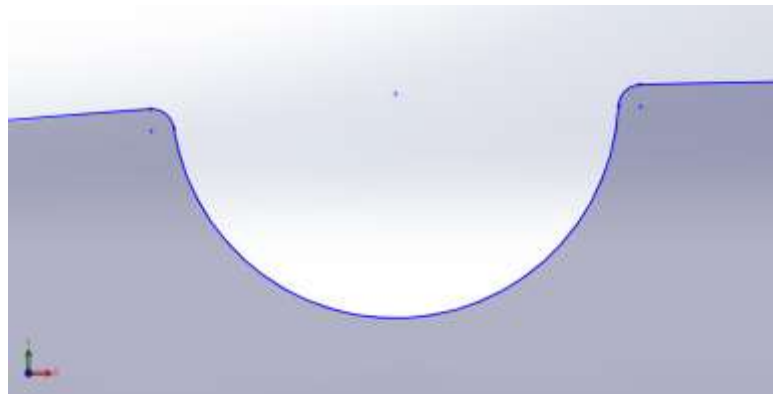


Figure 3.3: Oval 3 cavity with fillet size $c/10$

This process is repeated with different cavity ratio for each of the airfoil. Thus, each airfoil will have 240 different types of cavities in term of number, size, shape, and location. For example, figure 3.4 shows the airfoil E387 with 3 cavities at various positions (15c, 30c and 60c).

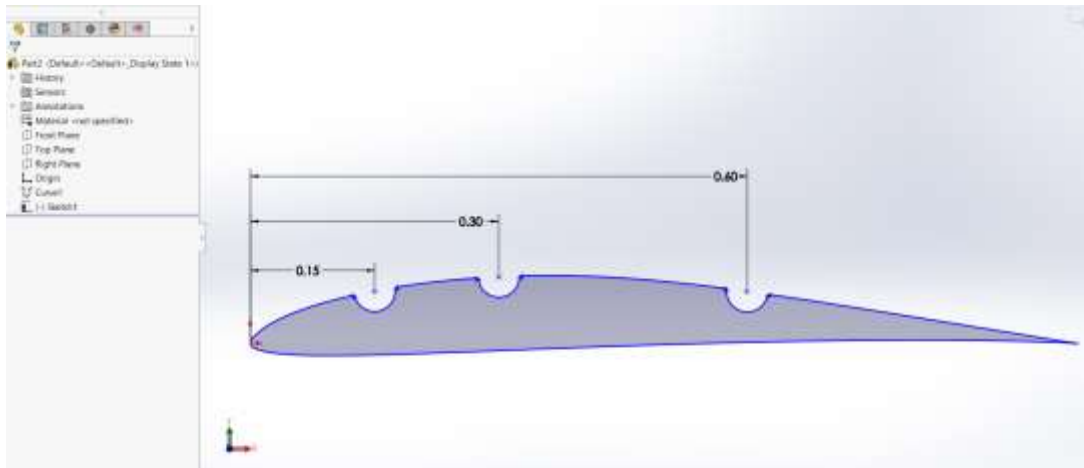


Figure 3.4: airfoil E387 with a triple cavity at 15c, 30c, 60c

Next, the finished airfoil design is aligned manually with point/dots to create the airfoil's new polar coordinates. Thus, the new airfoil outline can insert into the PROFILI software for further analysis. Figure 3.5 shows the points made on the modified E387 airfoil. The created points are converted into polar coordinates using the SOLIDWORKS macro function and save as a data table in Microsoft Excel. SOLIDWORKS macro is a series of commands and actions that can be stored and run within SOLIDWORKS. A series of commands is created in SOLIDWORKS macro to read and convert the points on the airfoil into polar coordinates and save them into a data sheet.